

Fabrication of zero-thermal-expansion $\text{ZrSiO}_4/\text{Y}_2\text{W}_3\text{O}_{12}$ sintered body

I. Yanase*, M. Miyagi, H. Kobayashi

Department of Applied Chemistry, Faculty of Engineering, Saitama University, 255 Shimoohkubo, Saitama 338-8570, Japan

Received 11 February 2009; received in revised form 16 May 2009; accepted 4 June 2009

Available online 1 July 2009

Abstract

We focused on the linear negative thermal expansion of $\text{Y}_2\text{W}_3\text{O}_{12}$ in a wide-temperature range and on the chemical stability of ZrSiO_4 in the fabrication of the composite material $\text{ZrSiO}_4/\text{Y}_2\text{W}_3\text{O}_{12}$ with a zero-thermal-expansion. The compact composed of $\text{Y}_2\text{W}_3\text{O}_{12}$ and ZrSiO_4 had a thermal shrinkage rate smaller than that of $\text{Y}_2\text{W}_3\text{O}_{12}$ and higher than that of ZrSiO_4 . SEM–EDX observation clarified that the $\text{ZrSiO}_4/\text{Y}_2\text{W}_3\text{O}_{12}$ sintered body fabricated at 1400 °C for 10 h had a microstructure composed of ZrSiO_4 and $\text{Y}_2\text{W}_3\text{O}_{12}$ grains, and XRD indicated that only ZrSiO_4 and $\text{Y}_2\text{W}_3\text{O}_{12}$ phases existed in the sintered body. The relative density of the $\text{ZrSiO}_4/\text{Y}_2\text{W}_3\text{O}_{12}$ sintered body reached 92%, which was larger than that of the ZrSiO_4 sintered body because $\text{Y}_2\text{W}_3\text{O}_{12}$ grains could be sintered at lower temperatures. The average linear thermal expansion coefficients of the $\text{ZrSiO}_4/\text{Y}_2\text{W}_3\text{O}_{12}$ sintered body were -0.4×10^{-6} and $-0.08 \times 10^{-6} \text{ } ^\circ\text{C}^{-1}$ in the temperature ranges from 25 to 500 °C and from 25 to 1000 °C, respectively, which showed an almost zero-thermal-expansion.

© 2009 Elsevier Ltd. All rights reserved.

Keywords: Composites; Thermal expansion; Yttrium tungstate; Zircon; TMA

1. Introduction

Recently, a zero- or near-zero-thermal-expansion property has been required for achieving high precision in modern industries, such as optics, microelectronics and energy transformation, to reduce measurement errors due to thermal deformation in the above fields.^{1–3} To meet the above requirements, zero- or near-zero-thermal-expansion materials have been studied. Composite materials have been of interest because they have an advantage in that one can control their thermal expansion coefficients by regulating the chemical compositions of their components.

For instance, ceramic composites fabricated by a reaction sintering process exhibited near-zero-thermal-expansion in the temperature range from RT to 773 K,⁴ in which $\text{Fe}_{0.2}\text{Sc}_{0.8}\text{Mo}_3\text{O}_{12}$ with a negative thermal expansion coefficient has been dispersed in a MoO_3 matrix with a positive thermal expansion coefficient. However, the composite exhibited positive thermal expansion above 773 K. $\text{BaO}-\text{Al}_2\text{O}_3-\text{B}_2\text{O}_3$ system glass-ceramics were fabricated^{5,6} as materials with a zero or even a negative thermal expansion coefficient,

which was smaller than that of glass-ceramics with β -spodumene⁷; however, their near-zero-thermal-expansion temperature region was narrow, that is, from RT to 373 K. $\text{ZrW}_2\text{O}_8-\text{ZrO}_2-\text{Al}_2\text{O}_3-\text{Al}_2(\text{WO}_4)_3$ system composites with a near-zero-thermal-expansion coefficient have been reported recently.⁸ However, the zero-thermal-expansion behavior changed discontinuously as a function of temperature owing to the structural phase transition of ZrW_2O_8 phase at approximately 430 K. Thus, it has been difficult to develop materials with a zero- or near-zero-thermal-expansion coefficient in a wide-temperature region. Moreover, ceramic materials without glass components are attractive for application at higher temperature.

Yttrium tungstate,^{9,10} $\text{Y}_2\text{W}_3\text{O}_{12}$, has a structural type of $\text{A}_2\text{M}_3\text{O}_{12}$ ^{11–14} with orthorhombic symmetry and exhibits an average negative thermal expansion coefficient of $-7.0 \times 10^{-6} \text{ K}^{-1}$ from 15 to 1373 K. The negative thermal expansion is considered to occur owing to transverse thermal vibrations¹² perpendicular to the Y–O–W linkage of the $\text{Y}_2\text{W}_3\text{O}_{12}$ unit cell. Three lattice parameters, namely, *a*-, *b*-, and *c*-axes of the unit cell, decreased continuously as functions of temperature, which results in a negative thermal expansion of the lattice volume of $\text{Y}_2\text{W}_3\text{O}_{12}$ over the above temperature range.⁹ $\text{Y}_2\text{W}_3\text{O}_{12}$ is easily synthesized because it has a more stable phase at RT than ZrW_2O_8 , which is necessary for quench

* Corresponding author. Tel.: +81 48 858 3720; fax: +81 48 858 3720.
E-mail address: yanase@apc.saitama-u.ac.jp (I. Yanase).

processes in the synthesis of ZrW_2O_8 powders^{15,16} and in the fabrication of composites including ZrW_2O_8 .⁸ Therefore, $\text{Y}_2\text{W}_3\text{O}_{12}$ is attractive as an additive to positive-thermal-expansion materials from the viewpoint of the fabrication of composite materials exhibiting a zero-thermal-expansion.

Zircon, ZrSiO_4 , is an interesting refractory material for high-temperature applications, having several excellent properties such as chemical stability, low thermal expansion, low thermal conductivity, and high resistance to thermal shock.^{17,18} In particular, the chemical stability of zircon is thought to be useful as a matrix phase in the fabrication of composite materials exhibiting zero-thermal-expansion because chemical reactions among components of the composites must be suppressed in the sintering of the composite materials. Therefore, in this study, we focused on the negative thermal expansion of $\text{Y}_2\text{W}_3\text{O}_{12}$ in a wide-temperature range and on the chemical stability of ZrSiO_4 , and fabricated the composite material $\text{Y}_2\text{W}_3\text{O}_{12}/\text{ZrSiO}_4$ with a zero-thermal-expansion.

2. Experimental procedure

2.1. Fabrication

$\text{Y}_2\text{W}_3\text{O}_{12}$ powders were prepared by solid-state reaction. Y_2O_3 (99.9% pure; Wako) and WO_3 (99.9% pure; Wako) powders were mixed in a stoichiometric ratio in ethanol by ball-milling for 24 h. The Y_2O_3 powders were dried in advance at 473 K for 5 h to remove absorbed water molecules. The as-dried mixed powders were shaped into cylindrical pellets of 10 mm diameter and 2 mm thickness by uniaxial pressing at 49 MPa, and then the compacts were heated at 1273 K for 5 h in an aluminum crucible. Here, the compacts were put on pre-prepared $\text{Y}_2\text{W}_3\text{O}_{12}$ powders to prevent the compact from reacting with the alumina crucible. The heated compacts were ground into powders with an agate mortar, and then the resulting $\text{Y}_2\text{W}_3\text{O}_{12}$ powders and commercial ZrSiO_4 powders (99% pure; Wako) were mixed with nominal compositions in ethanol by ball-milling for 24 h. The prepared powder mixtures of $\text{Y}_2\text{W}_3\text{O}_{12}$ and ZrSiO_4 were shaped into $5 \text{ mm} \times 5 \text{ mm} \times 50 \text{ mm}$ compacts by uniaxial pressing at 98 MPa, and the compacts were divided into four equal parts of approximately $5 \text{ mm} \times 5 \text{ mm} \times 12 \text{ mm}$ each. The compacts put on pre-prepared $\text{Y}_2\text{W}_3\text{O}_{12}$ powders in an alumina boat were sintered at temperatures of 1473–1673 K for 10 h in air at a heating rate of 5 K/min to fabricate $\text{ZrSiO}_4/\text{Y}_2\text{W}_3\text{O}_{12}$ sintered bodies.

2.2. Evaluation

The phases present in the powders and the sintered bodies were investigated by X-ray diffractometry (XRD; Rigaku Rad-C) using $\text{Cu K}\alpha$ radiation within the 2θ range of $15\text{--}40^\circ$. The bulk densities of ZrSiO_4 , $\text{Y}_2\text{W}_3\text{O}_{12}$, and $\text{ZrSiO}_4/\text{Y}_2\text{W}_3\text{O}_{12}$ sintered bodies were measured by the Archimedes method, with deionized water as the immersion medium. The relative densities of the sintered bodies were calculated using the theoretical densities (4.60 g/cm^3 for ZrSiO_4 , 4.698 g/cm^3 for $\text{Y}_2\text{W}_3\text{O}_{12}$, and 4.637 g/cm^3 for $\text{ZrSiO}_4/\text{Y}_2\text{W}_3\text{O}_{12}$). The relative density of the

$\text{ZrSiO}_4/\text{Y}_2\text{W}_3\text{O}_{12}$ sintered body with a zero-thermal-expansion was calculated from the mass ratio of $\text{ZrSiO}_4/\text{Y}_2\text{W}_3\text{O}_{12} = 1.660$.

The microstructures of the fractured surfaces of the sintered bodies were examined by scanning electron microscopy (SEM; Hitachi S4100) and energy dispersive X-ray analysis (EDX; Quantax400-125S). The thermal shrinkage behaviors of the compacts and the thermal expansion properties of the sintered bodies in the temperature range from 298 to 1273 K were investigated by thermomechanical analysis (TMA; Rigaku, Thermoplus TMA8310) at heating and cooling rates of 5 K/min.

3. Results and discussion

The thermal shrinkage behaviors of the compacts of $\text{Y}_2\text{W}_3\text{O}_{12}$, ZrSiO_4 , and $\text{ZrSiO}_4/\text{Y}_2\text{W}_3\text{O}_{12}$ in the temperature range from RT to 1473 K were investigated by TMA. The results are shown in Fig. 1. The $\text{Y}_2\text{W}_3\text{O}_{12}$ compact began to expand at approximately 323 K and reached around 0.8% in the expansion rate at 473 K, owing to the dehydration of $\text{Y}_2\text{W}_3\text{O}_{12}$.^{19,20} The thermal expansion rate of the $\text{Y}_2\text{W}_3\text{O}_{12}$ compact decreased gradually up to 1173 K, and then the compact began to shrink rapidly above 1173 K and reached a 6.0% shrinkage rate at 1473 K. The ZrSiO_4 compact showed almost no thermal shrinkage behavior in the temperature range from RT to 1173 K, although it shrank slightly above 1173 K. The $\text{ZrSiO}_4/\text{Y}_2\text{W}_3\text{O}_{12}$ compact showed thermal shrinkage with a shrinkage rate lower than that of $\text{Y}_2\text{W}_3\text{O}_{12}$ and higher than that of ZrSiO_4 . The expansion of the $\text{ZrSiO}_4/\text{Y}_2\text{W}_3\text{O}_{12}$ compact in the temperature range from RT to 1173 K was due to the removal of water molecules from $\text{Y}_2\text{W}_3\text{O}_{12}$ in the compact.

The relationships between the sintering temperature and relative density of the sintered bodies of $\text{ZrSiO}_4/\text{Y}_2\text{W}_3\text{O}_{12}$, ZrSiO_4 , and $\text{Y}_2\text{W}_3\text{O}_{12}$ are shown in Fig. 2. The $\text{Y}_2\text{W}_3\text{O}_{12}$ sintered body had a relative density of about 95% at 1473 K, which showed almost no change in the temperature range from 1473 to 1673 K. The high relative density corresponded to the thermal shrinkage

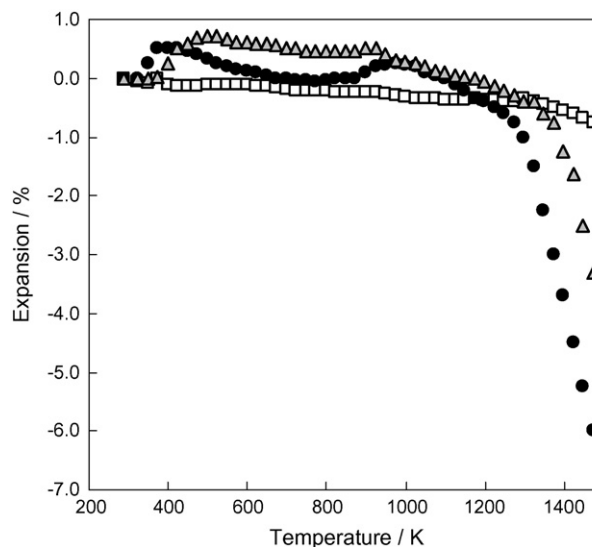


Fig. 1. Thermal shrinkage behaviors in temperature range of 298–1473 K for $\text{Y}_2\text{W}_3\text{O}_{12}$ (●), ZrSiO_4 (□), and $\text{Y}_2\text{W}_3\text{O}_{12}/\text{ZrSiO}_4$ (Δ; gray) compacts.

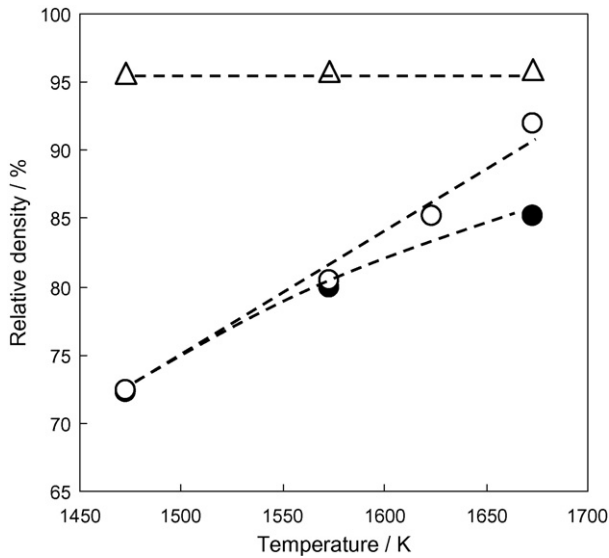


Fig. 2. Relationships between sintering temperature and relative density of Y₂W₃O₁₂/ZrSiO₄ (○), ZrSiO₄ (●), and Y₂W₃O₁₂ (□) sintered bodies fabricated at temperatures of 1473, 1573, and 1673 K for 10 h.

behavior of Y₂W₃O₁₂ shown in Fig. 1, suggesting that Y₂W₃O₁₂ could be sintered at low temperatures. The relative density of the ZrSiO₄ sintered body increased to about 85% at 1673 K, which was clearly lower than that of Y₂W₃O₁₂, and which corresponded to the low shrinkage rate of ZrSiO₄, as shown in Fig. 1. The relative density of the ZrSiO₄/Y₂W₃O₁₂ sintered body was almost equal to that of the ZrSiO₄ sintered body at 1473 and 1573 K, although the shrinkage rate increased gradually, suggesting that the existence of ZrSiO₄ grains suppressed the sintering among Y₂W₃O₁₂ grains. On the other hand, the relative densities at 1623 and 1673 K of the ZrSiO₄/Y₂W₃O₁₂ sintered body were larger than that of the ZrSiO₄ sintered body and increased to about 92% at 1673 K, indicating that the sintering among Y₂W₃O₁₂ grains proceeded with increasing the sintering temperature.

Fig. 3(a) and (b) shows the fractured surfaces of the Y₂W₃O₁₂ sintered body fabricated at 1673 K for 10 h. The densification of the Y₂W₃O₁₂ sintered body was recognized from the grains grown in the Y₂W₃O₁₂ sintered body. The thermal expansion property of the Y₂W₃O₁₂ sintered body was investigated by TMA. The result is shown in Fig. 4. The sintered

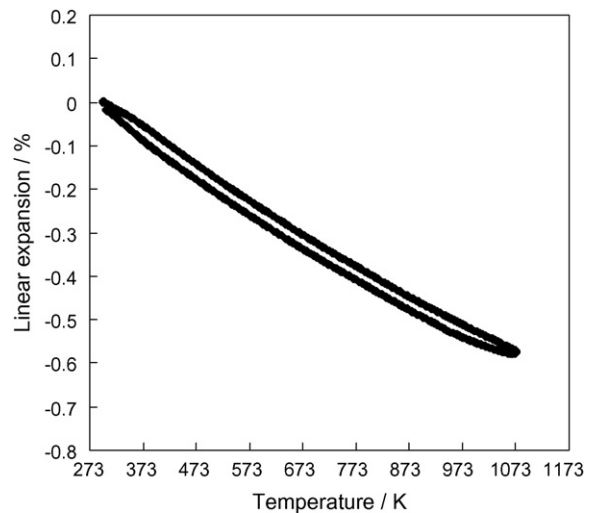


Fig. 4. Thermal expansion property in temperature range from 298 to 1073 K for Y₂W₃O₁₂ sintered body fabricated at 1673 K for 10 h.

body showed a negative thermal expansion in the temperature range of RT to 1273 K with a thermal expansion coefficient of $-7.63 \times 10^{-6} \text{ K}^{-1}$, which was almost similar to the report²¹ in the temperature range of 473–1073 K.

The fractured surfaces with the porous structure of the ZrSiO₄ sintered body, which were fabricated at 1673 K for 10 h, are shown in Fig. 5(a) and (b). The difference between the microstructures of the Y₂W₃O₁₂ and ZrSiO₄ sintered bodies implies that the Y₂W₃O₁₂ compact can be sintered at lower temperatures than the ZrSiO₄ compact, corresponding to the thermal shrinkage behaviors of these compacts shown in Fig. 1. The fractured surfaces of the ZrSiO₄/Y₂W₃O₁₂ sintered body, which were fabricated at 1673 K for 10 h, are shown in Fig. 6(a) and (b). The microstructure of the ZrSiO₄/Y₂W₃O₁₂ sintered body was clearly different from that of the ZrSiO₄ sintered body fabricated under the same conditions. From the microstructure of the ZrSiO₄/Y₂W₃O₁₂ sintered body, it was considered that the grain growth of Y₂W₃O₁₂ occupied space in the porous structure of the ZrSiO₄ sintered body, which resulted in the densification of the ZrSiO₄/Y₂W₃O₁₂ sintered body.

Fig. 7 shows a SEM image (a) and EDX composition maps (b)–(d) of the microstructure of the ZrSiO₄/Y₂W₃O₁₂ sintered body fabricated at 1673 K for 10 h. Map (b) is for the

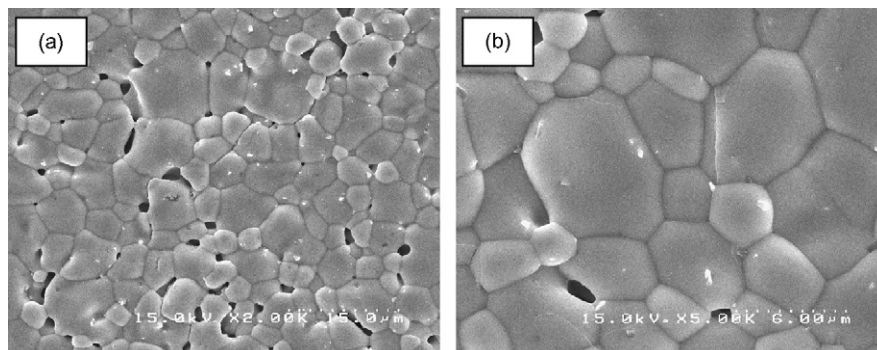


Fig. 3. SEM images of fractured surfaces of Y₂W₃O₁₂ sintered body fabricated at 1673 K for 10 h: (a) lower and (b) higher magnifications.

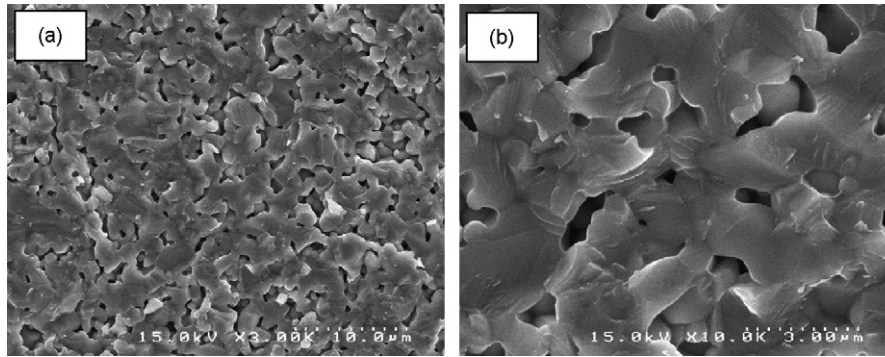


Fig. 5. SEM images of fractured surfaces of ZrSiO₄ sintered body fabricated at 1673 K for 10 h: (a) lower and (b) higher magnifications.

distribution of Y₂W₃O₁₂ and ZrSiO₄ grains, map (c) for that of ZrSiO₄ grains, and map (d) for that of Y₂W₃O₁₂ grains. It was observed that the ZrSiO₄/Y₂W₃O₁₂ sintered body had the microstructure composed of ZrSiO₄ and Y₂W₃O₁₂ grains, and that these ZrSiO₄ and Y₂W₃O₁₂ grains were dispersed. Fig. 8 shows the XRD pattern of the dense ZrSiO₄/Y₂W₃O₁₂ sintered body. Only Y₂W₃O₁₂ and ZrSiO₄ crystalline phases were observed in the sintered body, suggesting that the Y₂W₃O₁₂ and ZrSiO₄ grains did not react with each other in the sintering process owing to the chemical stability of ZrSiO₄.

The thermal expansion property with a slight hysteresis of the dense ZrSiO₄/Y₂W₃O₁₂ sintered body is shown in Fig. 9. The thermal expansion rate of the sintered body was almost zero in the temperature range of RT to 1273 K on heating, and the average thermal expansion coefficients were $-0.4 \times 10^{-6} \text{ K}^{-1}$ in the temperature range from 298 to 773 K and $-0.08 \times 10^{-6} \text{ K}^{-1}$ in the temperature range from 298 to 1273 K.

According to Kelly's rule using the volume ratios and thermal expansion coefficients of ZrSiO₄ and Y₂W₃O₁₂, the mass ratio of ZrSiO₄/Y₂W₃O₁₂ = 1.843 was considered to be necessary to fabricate a zero-thermal-expansion material, which means that in this study excess Y₂W₃O₁₂ was mixed with ZrSiO₄ to fabricate the sintered body with a zero-thermal-expansion because a zero-thermal-expansion material could be obtained when the mass ratio was 1.660. Indeed, when the mass ratio of ZrSiO₄/Y₂W₃O₁₂ was larger than 1.660, the thermal expansion rate of the ZrSiO₄/Y₂W₃O₁₂ sintered body increased, and

when it was smaller than 1.660, the thermal expansion rate of the sintered body decreased.

On the other hand, it was noted that the thermal expansion property exhibited a collapsed behavior over the temperature range from RT to 1073 K. This is because the mass ratio of ZrSiO₄/Y₂W₃O₁₂ for the fabrication of the compact was calculated using the average linear thermal expansion coefficients in the temperature range from RT to 1273 K although the coefficient of the Y₂W₃O₁₂ sintered body increased gradually with increasing temperature, as shown in Fig. 2. Furthermore, the thermal contraction in the temperature range from approximately 1073 to 1173 K and the slight positive thermal expansion above 1173 K were recognized in the thermal expansion property of the ZrSiO₄/Y₂W₃O₁₂ sintered body. Sumithra and Umarji reported that the Y₂W₃O₁₂ sintered body shows contraction due to creep at high temperatures^{19,20} and that creep brings about hysteresis in the thermal expansion of the Y₂W₃O₁₂ sintered body. Therefore, the contraction of the ZrSiO₄/Y₂W₃O₁₂ sintered body on heating was considered to occur due to the creep of Y₂W₃O₁₂ grains in the sintered body in the temperature range from approximately 1073 to 1173 K. The thermal expansion of the ZrSiO₄/Y₂W₃O₁₂ sintered body above 1173 K suggests that the positive thermal expansions induced by the ZrSiO₄ grains were not successfully suppressed by Y₂W₃O₁₂ grains owing to the creep of Y₂W₃O₁₂ grains.

Thus, the combination of the creep of Y₂W₃O₁₂ and the positive thermal expansion of ZrSiO₄ above 1073 K was con-

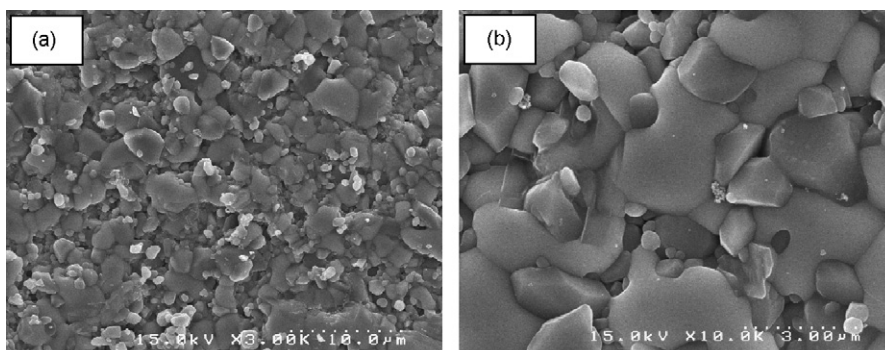


Fig. 6. SEM images of fractured surfaces of Y₂W₃O₁₂/ZrSiO₄ sintered body fabricated at 1673 K for 10 h: (a) lower and (b) higher magnifications.

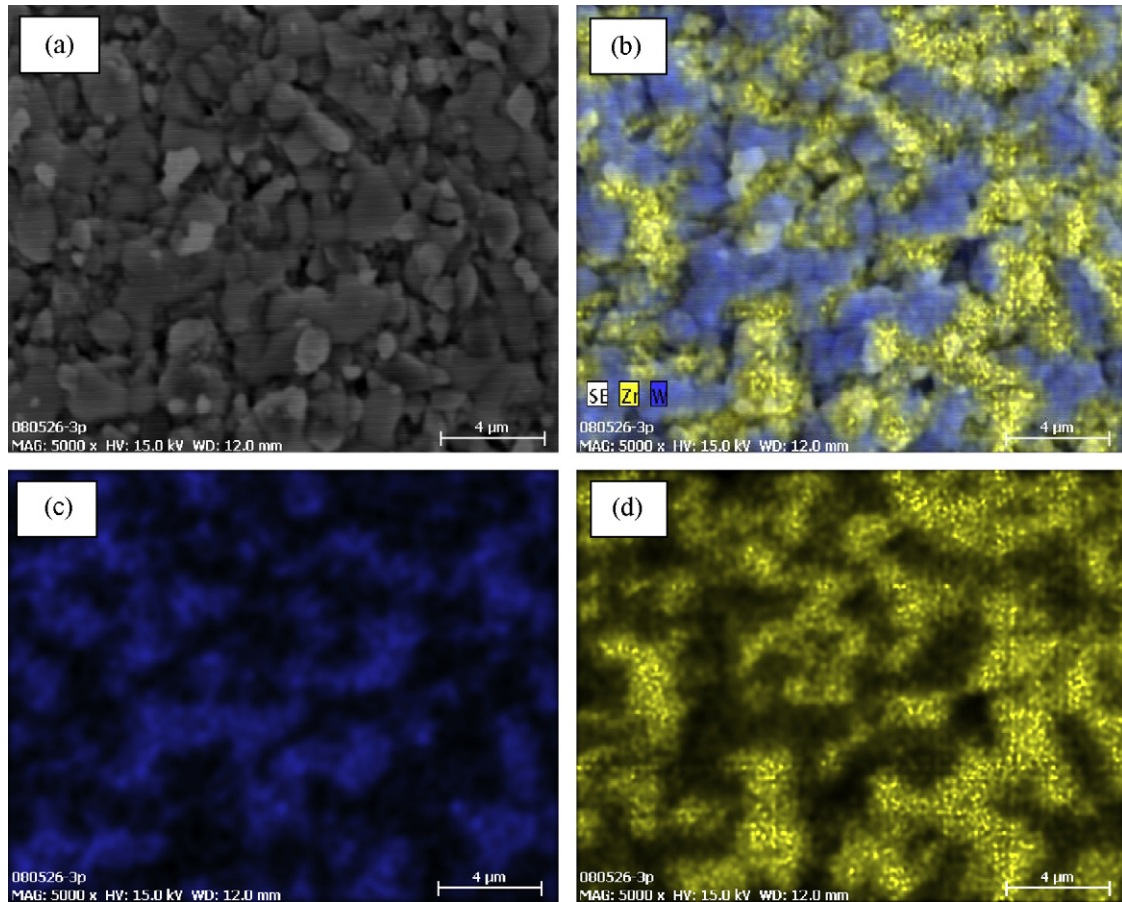


Fig. 7. SEM image (a) of $Y_2W_3O_{12}/ZrSiO_4$ sintered body and EDX composition maps: $Y_2W_3O_{12}$ and $ZrSiO_4$ grains (b), $ZrSiO_4$ grains (c), and $Y_2W_3O_{12}$ grains (d).

sidered to give rise to the slight hysteresis in the thermal expansion curve of the $ZrSiO_4/Y_2W_3O_{12}$ sintered body. However, the dense composite composed of $Y_2W_3O_{12}$ and $ZrSiO_4$ successfully showed an almost zero-thermal-expansion in the temperature range from RT to 1073 K on heating, showing that $ZrSiO_4$ can be an attractive candidate in the fabrication of zero-thermal-expansion materials including negative-thermal-expansion substances.

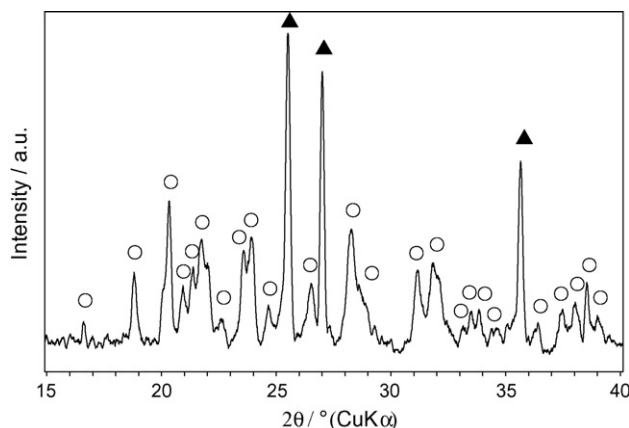


Fig. 8. XRD pattern of $Y_2W_3O_{12}/ZrSiO_4$ sintered body fabricated at 1673 K for 10 h: $Y_2W_3O_{12}$ (○) and $ZrSiO_4$ (▲).

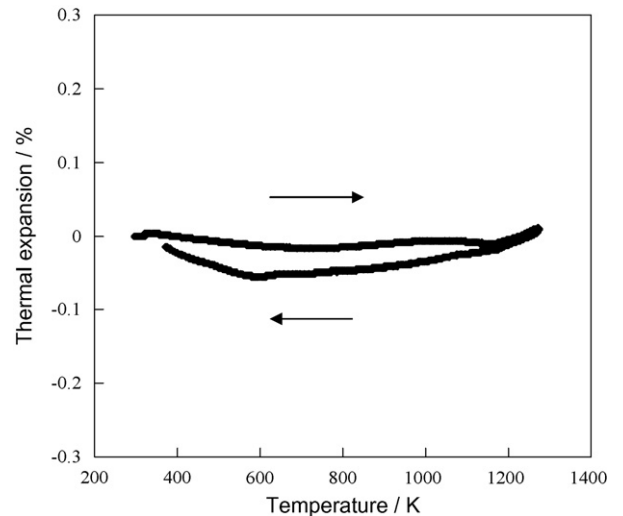


Fig. 9. Thermal expansion property in temperature range of 298–1273 K for $Y_2W_3O_{12}$ sintered body fabricated at 1673 K for 10 h.

4. Conclusions

Composites of $Y_2W_3O_{12}$ and $ZrSiO_4$ were fabricated by sintering at 1673 K for 10 h. The fabricated $Y_2W_3O_{12}/ZrSiO_4$ sintered body had a dense microstructure, and $ZrSiO_4$ and

$\text{Y}_2\text{W}_3\text{O}_{12}$ grains were observed in the microstructure of the dense sintered body. Its XRD pattern indicated that $\text{Y}_2\text{W}_3\text{O}_{12}$ and ZrSiO_4 grains did not react with each other in during sintering. The average linear thermal expansion coefficients of the sintered body were $-0.4 \times 10^{-6} \text{ K}^{-1}$ in the temperature range from 298 to 773 K and $-0.08 \times 10^{-6} \text{ K}^{-1}$ in the temperature range from 298 to 1273 K, showing an almost zero-thermal-expansion.

Acknowledgement

This study was supported by Tanigawa Thermal Technology Foundation in Japan.

References

1. Yang, X., Cheng, X., Yan, X., Yang, J., Fu, T. and Qiu, J., Synthesis of $\text{ZrO}_2/\text{ZrW}_2\text{O}_8$ composites with low thermal expansion. *Compos. Sci. Technol.*, 2007, **67**, 1167–1171.
2. Niwa, E., Wakamoto, S., Ichikawa, T., Wang, S., Hashimoto, T., Takahashi, K. et al., Preparation of dense $\text{ZrO}_2/\text{ZrW}_2\text{O}_8$ cosintered ceramics with controlled thermal expansion coefficients. *J. Ceram. Soc. Jpn.*, 2004, **112**, 271–275.
3. Namba, Y., Takehara, H. and Nagano, Y., Fracture strength of zero-thermal-expansion glass-ceramics for ultra-precision components. *CIRP Ann. Manuf. Technol.*, 2001, **50**, 239–242.
4. Tran, K. D., Groshens, T. J. and Nelson, J. G., Fabrication of near-zero thermal expansion $(\text{Fe}_x\text{Sc}_{1-x})_2\text{Mo}_3\text{O}_{12}-\text{MoO}_3$ ceramic composite using the reaction sintering process. *Mater. Sci. Eng. A*, 2001, **303**, 234–240.
5. Tauch, D. and Russel, C., Glass-ceramics with zero thermal expansion in the system $\text{BaO}/\text{Al}_2\text{O}_3/\text{B}_2\text{O}_3$. *J. Non-Cryst. Solids*, 2005, **351**, 2294–2298.
6. Tauch, D. and Russel, C., Glass-ceramics in the system $\text{BaO}/\text{TiO}_2(\text{ZrO}_2)/\text{Al}_2\text{O}_3/\text{B}_2\text{O}_3$ and their thermal expansion. *J. Non-Cryst. Solids*, 2007, **353**, 2109–2114.
7. Sakamoto, A., Asano, H., Wada, M., Yamamoto, S. and Nishii, J., Mechanical and optical properties of silica glass optical fiber with low-expansion glass-ceramic jacket. *J. Ceram. Soc. Jpn.*, 2003, **111**, 640–644.
8. Sun, L., Sneller, A. and Kwon, P., ZrW_2O_8 -containing composites with near-zero coefficient of thermal expansion fabricated by various methods: comparison and optimization. *Compos. Sci. Technol.*, 2008, **68**, 3425–3430.
9. Forster, P. M. and Sleight, A. W., Negative thermal expansion in $\text{Y}_2\text{W}_3\text{O}_{12}$. *Int. J. Inorg. Mater.*, 1999, **1**, 123–127.
10. Koltsova, T. N., X-ray diffraction study of $\text{Y}_2\text{W}_3\text{O}_{12} \cdot 3\text{H}_2\text{O}$. *Inorg. Mater.*, 2001, **37**, 1175–1177.
11. Wu, M. M., Peng, J., Cheng, Y. Z., Wang, H., Yu, Z. X., Chen, D. F. et al., Structural and thermal expansion properties of solid solution $\text{Nd}_{2-x}\text{Eu}_x\text{W}_3\text{O}_{12}$ ($0.0 \leq x \leq 0.6$ and $1.5 \leq x \leq 2.0$). *Solid-State Sci.*, 2006, **8**, 665–670.
12. Evans, J. S. O., Mary, T. A. and Sleight, A. W., Negative thermal expansion in $\text{Sc}_2(\text{WO}_4)_3$. *J. Solid-State Chem.*, 1998, **137**, 148–160.
13. Forster, P. M., Yokochi, A. and Sleight, A. W., Enhanced negative thermal expansion in $\text{Lu}_2\text{W}_3\text{O}_{12}$. *J. Solid-State Chem.*, 1998, **140**, 157–158.
14. Evans, J. S. O., Mary, T. A. and Sleight, A. W., Negative thermal expansion materials. *Phys. B*, 1998, **241–243**, 311–316.
15. Lommens, P., Meter, C. De., Bruneel, E., Buysser, K. D., Driessche, I. V. and Hoste, S., Synthesis and thermal expansion of $\text{ZrO}_2/\text{ZrW}_2\text{O}_8$ composites. *J. Eur. Ceram. Soc.*, 2005, **25**, 3605–3610.
16. Morito, Y., Wang, S., Oshima, Y., Uehara, T. and Hashimoto, T., Preparation of dense negative-thermal expansion oxide by rapid quenching of ZrW_2O_8 melt. *J. Ceram. Soc. Jpn.*, 2002, **110**, 544–548.
17. Terki, R., Bertrand, G. and Aourag, H., Full potential investigations of structural and electronic properties of ZrSiO_4 . *Microelectron. Eng.*, 2005, **81**, 514–523.
18. Veytizou, C., Quinson, J. F. and Jorand, Y., Preparation of zircon bodies from amorphous precursor powder synthesized by sol-gel processing. *J. Eur. Ceram. Soc.*, 2002, **22**, 2901–2909.
19. Sumithra, S. and Umarji, A. M., Hygroscopicity and bulk thermal expansion in $\text{Y}_2\text{W}_3\text{O}_{12}$. *Mater. Res. Bull.*, 2005, **40**, 167–176.
20. Sumithra, S. and Umarji, A. M., Dilatometric studies of $\text{Y}_2\text{W}_3\text{O}_{12}$ with added Al_2O_3 . *Proc. Indian Acad. Sci.*, 2003, **115**, 695–701.
21. Sumithra, S., Tyagi, A. K. and Umarji, A. M., Negative thermal expansion in $\text{Eu}_2\text{W}_3\text{O}_{12}$ and $\text{Yb}_2\text{W}_3\text{O}_{12}$ by high temperature X-ray diffraction. *Mater. Sci. Eng. B*, 2005, **116**, 14–18.